Supplementary Material for "Single-molecule FRET analysis of DNA binding and bending by yeast HMGB protein Nhp6A" by Coats et al.

Supplementary Results

Nhp6A:DNA interactions in ensemble binding experiments

With any single-molecule FRET experiment, it is important to ensure that the behavior observed at the single-molecule level is consistent with ensemble observations. Ensemble fluorescence anisotropy experiments were therefore designed to characterize the binding and dissociation of yNhp6A in complex with an 18-bp dsDNA target in solution. The 18-bp duplex target sequence used in the fluorescence anisotropy experiments was identical to the sequence of the linear_18a duplex used in smFRET experiments reported in the main manuscript. In the fluorescence anisotropy DNA construct, a TAMRA dye was attached to one terminus of the duplex to serve as the fluorescent reporter, and this anisotropy probe was termed TAMRA_linear_18a.

yNhp6A protein (0-330 nM) was titrated into a 5 nM solution of TAMRA_linear_18a, and the anisotropy of the TAMRA dye was determined at each yNhp6A concentration. The relative anisotropy value (ΔAnisotropy; anisotropy value of the yNhp6A-bound TAMRA_linear_18a minus the anisotropy value of the unbound TAMRA_linear_18a) was then determined at each protein concentration. The relative anisotropy versus yNhp6A data was then fit by nonlinear regression to an equation (see Supplementary Materials and Methods) representing a 1:1 binding isotherm to estimate the equilibrium dissociation constant, K_D (**Supplementary Fig. S1A**). In this binding experiment, the K_D estimate was ~1.8 ± 0.6 nM, in agreement with smFRET results.

Anisotropy measurements required a minimum concentration of 5 nM TAMRA-labeled probe. Because the K_D estimate is lower than this probe DNA concentration, there is some uncertainty in this estimate. Nonetheless, this experiment provides a control to ensure that the ensemble equilibrium dissociation constant is in a range consistent with the smFRET data.

To assess yNhp6A ensemble dissociation rates, 50 nM yNhp6A was incubated with 5 nM TAMRA_linear_18a, and the anisotropy of the complex was measured in steady state (**black line in Supplementary Fig. S1B**) for the indicated times prior to addition of a 40-fold concentration excess of unlabeled dsDNA target (**red arrow and line in Supplementary Fig. S1B**). The sample anisotropy dropped within seconds to an anisotropy value corresponding to the TAMRA_linear_18a alone in solution (**dotted line in Supplementary Fig. S1B**), indicating that yNhp6A dissociates rapidly from the TAMRA_linear_18a probe under these conditions. This result is consistent with the smFRET results reported in the main manuscript, which indicate that yNhp6A dissociates from 18 bp dsDNA within seconds.

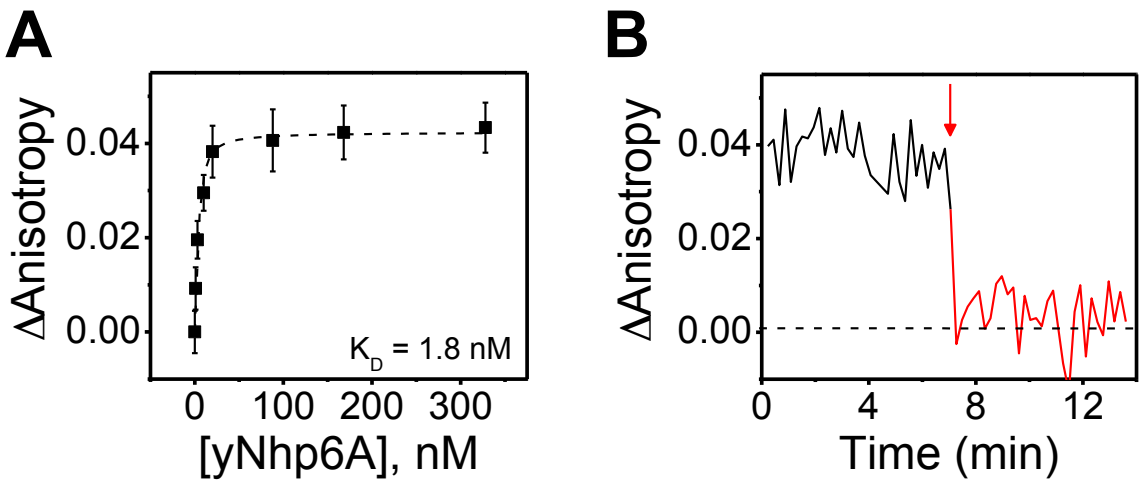

Supplementary Figure S1

Ensemble yNhp6A:DNA binding studies (A) Relative anisotropy values (ΔAnisotropy) of TAMRA dyes conjugated to dsDNA are plotted at increasing yNhp6A concentrations (black squares), and the points were fit to a 1:1 binding isotherm to estimate the equilibrium dissociation constant (K_D; black dotted line). (B) yNhp6A (50 nM) was pre-bound to 5 nM TAMRA-labeled dsDNA (TAMRA_linear_18a), and the relative anisotropy value was measured as a function of time (black line). Then, excess unlabeled dsDNA (the concentration of the unlabeled dsDNA was 40x that of the TAMRA_linear_18a) was added to the reaction (red arrow), and the relative anisotropy was measured over time (red line).

Determination of yNhp6A-induced bending angles

FRET efficiency (E_{FRET}) was plotted as a function of distance between the dyes R (**Supplementary Fig. S2A**). This plot was generated from $E_{FRET} = (1+R^6/R_0^6)^{-1}$, using a R_0 value of 60.1 Å—which was determined previously for the Cy3-Cy5 FRET pair conjugated to DNA (19,29). Then, the E_{FRET} versus R data was used to generate a plot of the FRET efficiency versus estimated bending angles (θ) for each substrate (**Supplementary Fig. S2B**) using the law of cosines: $\theta = \cos^{-1}\left[\frac{2\left(\frac{1}{2}R_{unbent}\right)^2 - (R_{bent})^2}{2\left(\frac{1}{2}R_{unbent}\right)^2}\right]$ (R_{unbent} is the distance between dyes when the DNA is unbent and R_{bent} is the distance between the dyes when the DNA is bent). The plot of E_{FRET} versus θ reports on the internal angles between the ends of the DNA molecules in the absence and presence of yNhp6A (**Supplementary s. S2B**). In the main manuscript, yNhp6A-induced bending angles (yNhp6A bends Linear_18a and Linear_18b by a ~60° external angle and bends Bulge_18a by a ~45° external angle) were determined by subtracting the angle between the ends of the bent DNA ($\theta_{Linear\_18a} = \theta_{Linear\_18b} = 120°$, $\theta_{Bulge\_18a} = 135°$) from the angle between the ends of the unbent DNA ($\theta_{Linear\_18a} = \theta_{Linear\_18b} = \theta_{Bulge\_18a} = 180°$) (**Supplementary Fig. S2C**). It should be pointed out that the angle determinations described here were calculated with the simplifying assumption that the relative orientation of the Cy3-Cy5 FRET pair was similar before and after protein-induced bending which is a detail that could have a small effect on the observed E_{FRET} values and thus the calculated R and θ values (19). However, the calculated external bending angles for yNhp6A in complex with the homoduplex DNA (~60°) is in agreement with

the external bending angles determined via AFM (~60°) (11), gel electrophoresis (~63°) (20), and NMR (~70°) (4), so any error in measurement due to the relative orientation of the dyes is small. Furthermore, the model presented in this work is not dependent on the precise angles of the bent protein-DNA complexes but rather the observation that discrete binding and dissociation events lead to increased flexibility of duplex DNA.

.

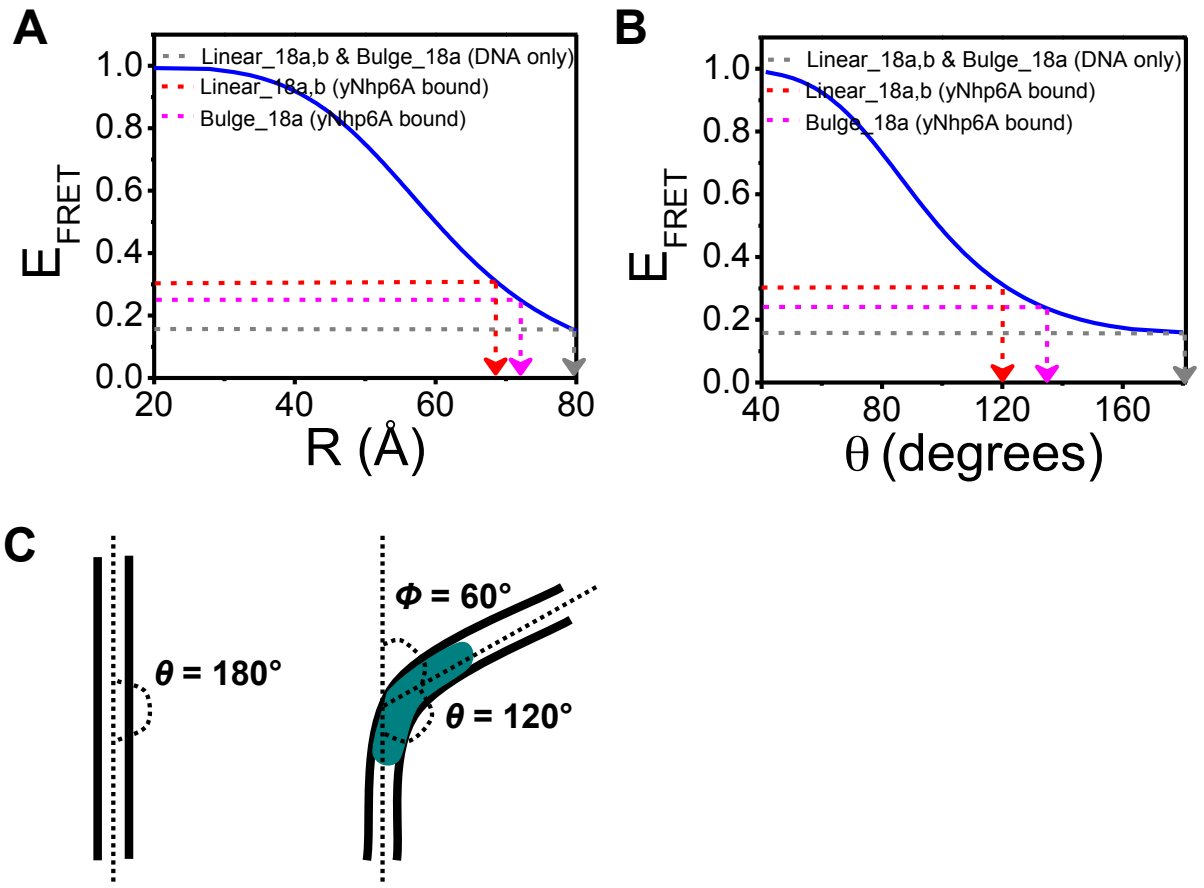

Supplementary Figure S2

Determination of yNhp6A-induced bending angles for the 18 bp targets (A) A plot of the FRET efficiency (E_{FRET}) versus distance between the donor and acceptor fluorophores (R) is shown (blue line). (B) A plot of E_{FRET} versus the internal angle between the fluorophores (θ) is given (blue line). (C) The schematic diagrams show the conventions described in the text. The left figure represents an unbent DNA molecule that has an internal angle between fluorophores of θ = 180°. The right figure illustrates a yNhp6A-bend DNA molecule that has an internal angle between fluorophores of θ = 120° and an external bending angle of Φ = 60°.

smFRET data for yNhp6A binding to 15 bp DNA targets

The smFRET experiments described in the main work involve 18 bp long DNA duplexes (two different homoduplex targets and one bulged target). smFRET experiments were also performed with shorter, 15 bp long DNA duplexes (one homoduplex target and one bulged target) with labeling and immobilization schemes identical to those of the longer duplexes, and the experiments with the 15 bp DNA targets were performed as described for the 18 bp targets detailed in the main work. yNhp6A was observed to bind the 15 bp homoduplex DNA target (linear_15a) and 15 bp bulged target (bulge_15a) with affinity, dynamics, and bend angles similar to that for the 18 bp homoduplex DNA targets (linear_18a and linear_18b, respectively) (**supplementary Figs. S3, S4, and S5**).

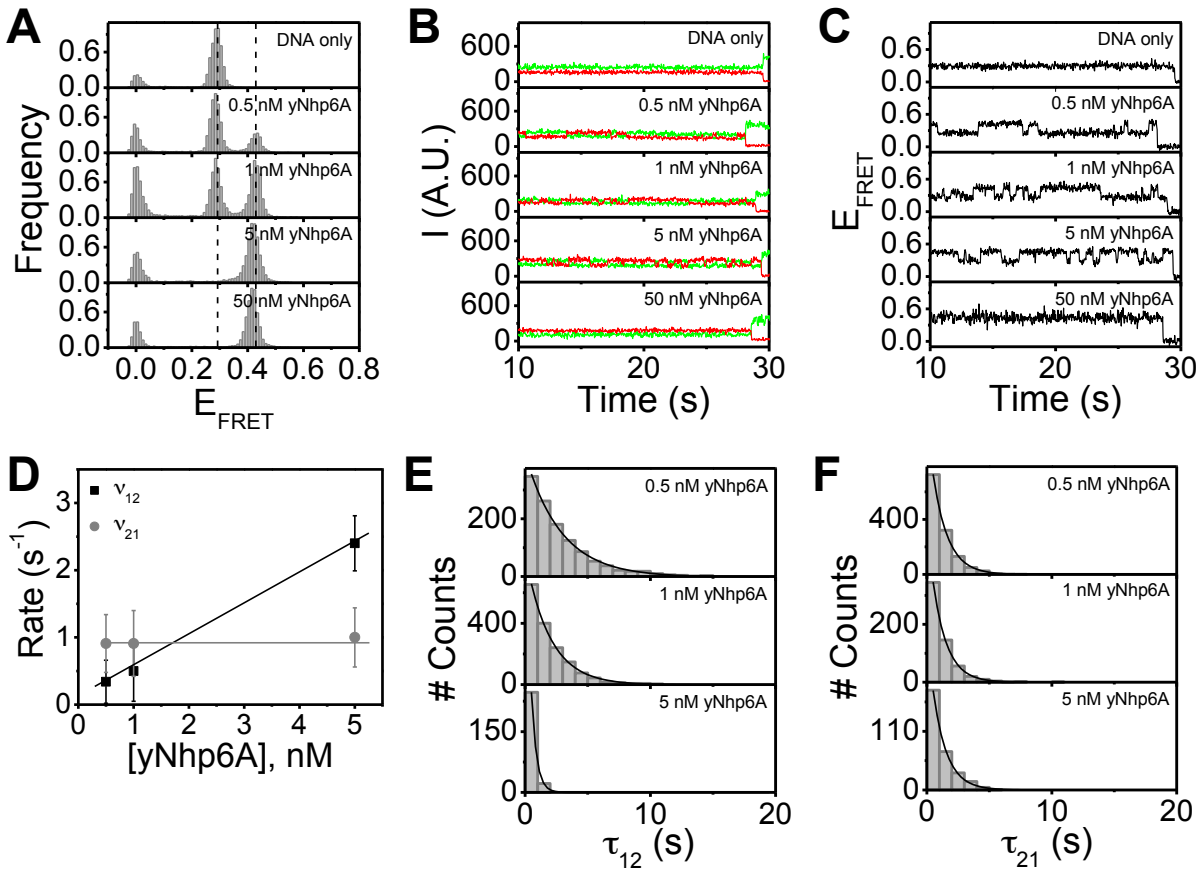

Supplementary Figure S3

Studies of yNhp6A binding to 15 bp homoduplex DNA (linear_15a) (A) FRET efficiency histograms in the absence and presence of yNhp6A, as indicated; (B-C) Single-molecule intensity and corresponding FRET efficiency time traces in the absence and presence of yNhp6A; (D) Transition rates as a function of yNhp6A concentration (v_{12} is the transition rate from the low FRET (unbound) state to the high FRET (bound) state and v_{21} is the transition rate from the high FRET (bound) state to the low FRET (unbound) state); (E-F) Dwell time histograms for the low FRET (τ_{12}) and high FRET (τ_{21}) states at 0.5, 1, and 5 nM yNhp6A.

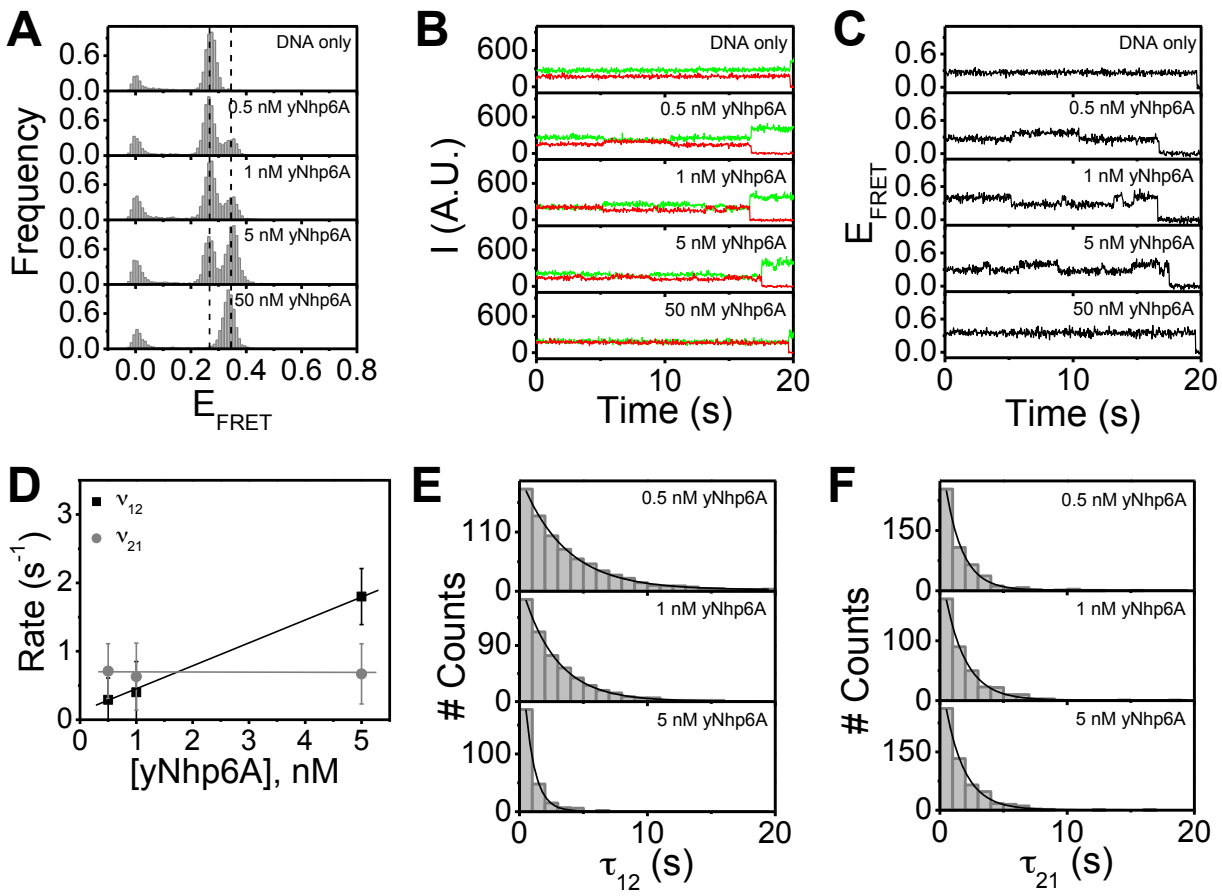

Supplementary Figure S4

Studies of yNhp6A binding to 15 bp bulged DNA (bulge_15a). (A) FRET efficiency histograms in the absence and presence of yNhp6A, as indicated; (B-C) Single-molecule intensity and corresponding FRET efficiency time traces in the absence and presence of yNhp6A; (D) Transition rates as a function of yNhp6A concentration (v_{12} is the transition rate from the low FRET (unbound) state to the high FRET (bound) state and v_{21} is the transition rate from the high FRET (bound) state to the low FRET (unbound) state); (E-F) Dwell time histograms for the low FRET (τ_{12}) and high FRET (τ_{21}) states at 0.5, 1, and 5 nM yNhp6A.

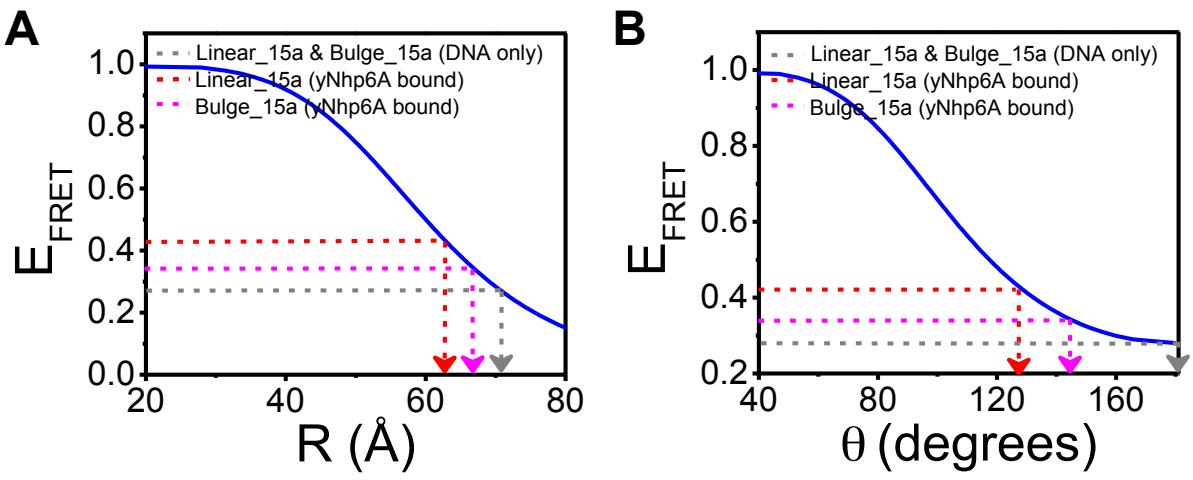

Supplementary Figure S5

Determination of yNhp6A-induced bending angles for the 15 bp targets (A) A plot of the FRET efficiency (E_{FRET}) versus distance between the donor and acceptor fluorophores (R) is shown (blue line). (B) A plot of E_{FRET} versus the internal angle between the fluorophores (θ) is given (blue line).

Supplementary Materials and Methods

Fluorescence anisotropy experiments

Fluorescence anisotropy experiments were performed in a buffer containing 10 mM HEPES pH 7.5, 100 mM NaCl, 1 mM $MgCl_2$, 5% glycerol, and 0.1 mg/mL BSA using a Fluoromax-4 fluorometer (Jobin-Yvon, Horiba). All experiments were at room temperature (~22°C) in a quartz fluorometer cell (Starna Cells, Inc.). The TAMRA probe was excited at 540 nm, and the fluorescence emission detected at 583 nm. In the binding experiment, 0-330 nM yNhp6A was incubated for 5 min with 5 nM TAMRA-labeled dsDNA and the steady state anisotropy value was measured for 10 min. Relative anisotropy versus yNhp6A concentration was plotted and fit by nonlinear regression to the following equation reflecting a 1:1 binding isotherm to estimate the equilibrium dissociation constant, K_D:

$$Y_{yNhp6A} = \left(\frac{K_D + [yNhp6A] + [DNA] - \sqrt{(K_D + [yNhp6A] + [DNA])^2 - 4[yNhp6A][DNA]}}{2[DNA]} \right) Y_{\max}$$

where [yNhp6A] is the yNhp6A concentration, [DNA] is the TAMRA-labeled dsDNA probe concentration, Y_{max} is the maximum relative anisotropy value at yNhp6A saturation, and Y_{yNhp6A} is relative anisotropy value at a given [yNhp6A]. Anisotropy measurements are averages of three determinations at each concentration. In the competition experiment, 50 nM yNhp6A was incubated for 5 min with 5 nM TAMRA-labeled dsDNA, and 2 μM unlabeled dsDNA was then added to the cuvette.

The oligonucleotides used in the ensemble experiments were purchased from Integrated DNA Technologies (IDT). Complementary strands were annealed in a 1:1.2 ratio by heating the strands at 80°C for three minutes and cooling them slowly to room temperature, and the DNA was purified using PAGE. The sequences are as follows:

TAMRA_Linear_18a:

Strand A: 5'-TGG CGA CGG CAG CGA GGC/TAMRA/-3'

Strand B: 5'-GCC TCG CTG CCG TCG CCA-3'

Unlabeled_Linear_18a:

Strand A: 5'-TGG CGA CGG CAG CGA GGC-3'

Strand B: 5'-GCC TCG CTG CCG TCG CCA-3'

Single-molecule experiments

The sequences of the oligonucleotides used to construct the 15 bp single-molecule FRET targets are as follows:

Linear_15a:

Strand A: 5'-/Cy3/CGA CGG CAG CGA GGC-3'

Strand B: 5'-/Cy5/GCC TCG CTG CCG TCG CCA TTT TTT TTT TTT TTT/Biotin/-3'

Bulge_15a:

Strand A: 5'-/Cy3/CGA CGG CAA AGC GAG GC-3'

Strand B: 5'-/Cy5/GCC TCG CTG CCG TCG CCA TTT TTT TTT TTT TTT/Biotin/-3'

Supplementary References

4. Masse, J.E., Wong, B., Yen, Y.M., Allain, F.H.T., Johnson, R.C. and Feigon, J. (2002) The S. cerevisiae architectural HMGB protein NHP6A complexed with DNA: DNA and protein conformational changes upon binding. *J. Mol. Biol.*, **323**, 263-284.
11. Zhang, J.Y., McCauley, M.J., Maher, L.J., Williams, M.C. and Israeloff, N.E. (2012) Basic N-Terminus of Yeast Nhp6A Regulates the Mechanism of Its DNA Flexibility Enhancement. *J. Mol. Biol.*, **416**, 10-20.
19. Iqbal, A., Arslan, S., Okumus, B., Wilson, T.J., Giraud, G., Norman, D.G., Ha, T. and Lilley, D.M.J. (2008) Orientation dependence in fluorescent energy transfer between Cy3 and Cy5 terminally attached to double-stranded nuclelic acids. *Proc. Natl. Acad. Sci. U. S. A.*, **105**, 11176-11181.
20. Tang, L.J., Li, J., Katz, D.S. and Feng, J.A. (2000) Determining the DNA bending angle induced by non-specific high mobility group-1 (HMG-1) proteins: A novel method. *Biochemistry*, **39**, 3052-3060.
29. Murphy, M.C., Rasnik, I., Cheng, W., Lohman, T.M. and Ha, T.J. (2004) Probing single-stranded DNA conformational flexibility using fluorescence spectroscopy. *Biophys. J.*, **86**, 2530-2537.